2

CONF-9104331--1

UCRL-JC--108348

DE92 006882

Ablation Gas Dynamics of Low-Z Materials Illuminated by Soft X-Rays

S. P. Hatchett
Lawrence Livermore National Laboratory
Livermore, CA

This was prepared to be presented at the
Lecture Series on Inertial Fusion
Department of Astrophysical Sciences
Princeton, NJ
April 1991

September 6, 1991

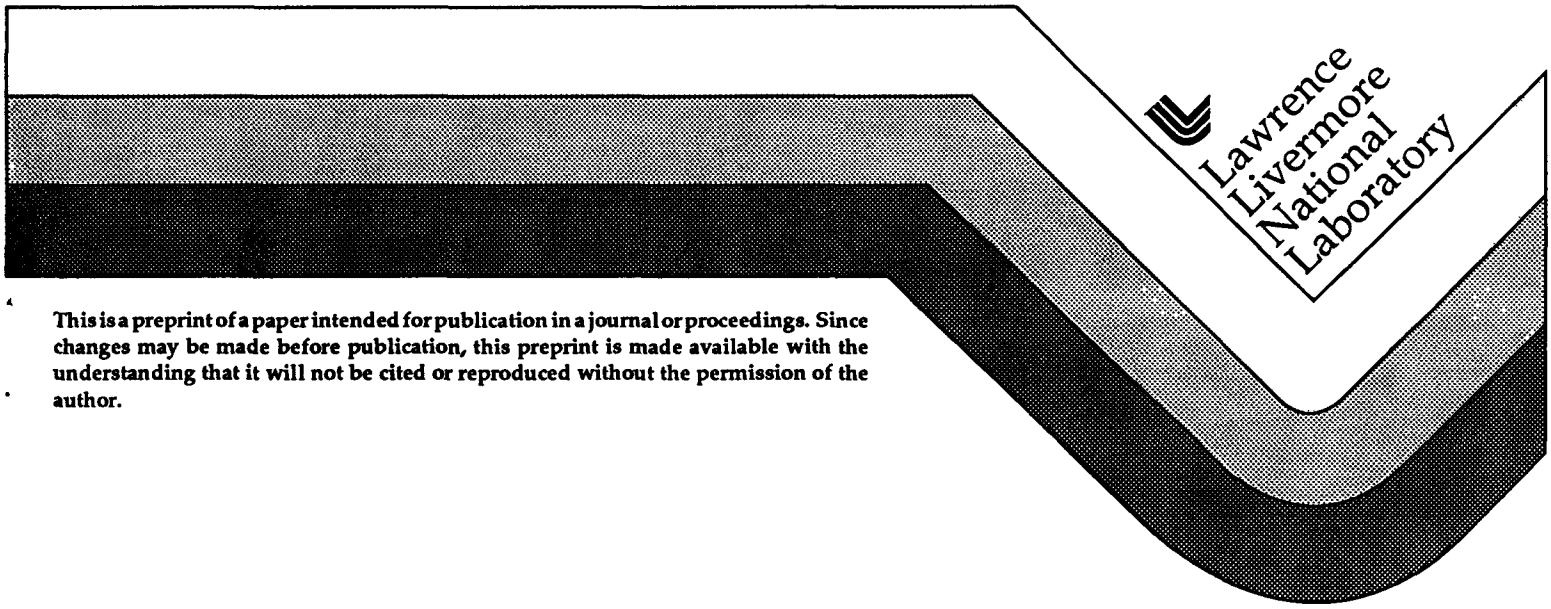

DISCLAIMER

ABLATION GAS DYNAMICS OF LOW-Z MATERIALS ILLUMINATED BY SOFT X-RAYS

Stephen P. Hatchett

I. INTRODUCTION

Though many of our results will have much greater generality, the main purpose of this paper is to provide a simple, accurate, physical theory of what happens when a Planckian spectrum of soft X-rays is incident on one side of a slab of initially cold, dense material, of small nuclear charge Z. Our approach will be to consider in some detail the idealized situation shown in Fig. 1. A semi-infinite ($x \leq 0$) slab of initially cold ($T < 300$ K), dense ($\rho \sim 1 - 10$ g/cc), low-Z ($Z < 5$) material is suddenly subjected at time $t = 0$ and thereafter to radiation incoming from $x = +\infty$ with a specific intensity in directions toward the slab that is Planckian, characterized by a black-body temperature, T_R in the soft X-ray region.

We naturally expect the incident X-rays to be absorbed by the slab material and heat it up, and that hot ($T \approx T_R$) material will blow off the face of the slab. The problem of what happens after enough material has been heated that the hot material is quite optically thick to incident X-rays has already been solved to some extent by the theory of "Marshak waves."[1] However, for the case of low-Z materials the hot portion will be fully ionized so that its opacity will be relatively low, and there may be a significant period of time (of order tens of nanoseconds) during which the hot blowoff has a Planck mean optical depth, τ_P, of less than a few. Radiation will not then diffuse toward cold material but will be more or less incident directly on it. We shall concern ourselves here with these "early" times.

We expect the following general features of the resulting gas dynamic flow. The X-rays will be absorbed in a boundary between hot and cold material -- at a radiative heat front, or what we shall simply call a heat front. This heat front will be rather narrow having a thickness of about one Planck mean free path (photon mfp averaged with respect to $B_\nu(T_R)$) in un-ionized, dense material. Assuming the flux of radiation driving this heat front is steady or slowly varying, we expect the heat front itself to be nearly steady. Depending on how fast the heat front is able to propagate into the slab, a shock wave may or may not break off and propagate ahead of it. Behind the heat front will be some sort of rarefaction flow of hot, ionized material into the vacuum. If its

opacity does not get too low, the hot gas will remain coupled to the radiation bath in which it is immersed, and will be approximately isothermal with $T \approx T_R$.

In the next section we shall develop the theory of heat fronts driven by a steady flux of radiation and then use that theory and the physical conditions of our model problem to construct explicit solutions for the gas dynamic flow. Following that, in Section III we shall modify our theory to introduce some time-dependent effects and discuss such things as conditions before a steady heat front is set up, so called "transonic" fronts, and albedo affects.

II. GAS FLOWS DRIVEN BY STEADY RADIATIVE HEAT FRONTS

Steady Heat Fronts: In the same manner as is usually used to discuss shock fronts, we shall write the equations for conservation of mass, momentum, and energy in a frame in which the heat front is motionless. Since we are solving a one dimensional problem, all velocities are assumed to be perpendicular to the heat front. Let subscript 1 refer to quantities immediately upstream of the heat front and subscript 2 to quantities immediately downstream. On the assumption that the heat front is steady we can integrate the differential equations of motion across it and obtain:

$$\rho_1 u_1 = \rho_2 u_2 \tag{1}$$

$$P_1 + \rho_1 u_1^2 = P_2 + \rho_2 u_2^2 \tag{2}$$

$$h_1 + \frac{1}{2}u_1^2 + \frac{F}{\rho u} = h_2 + \frac{1}{2}u_2^2 \tag{3}$$

(equations representing the conservation of mass, momentum, and energy, respectively), where ρ is density, u is velocity, P is pressure, h is enthalpy per unit mass and F is a flux of energy absorbed and thermalized at the front.

To place heat fronts in the context of other gas dynamic fronts, we note that these are, of course, just the familiar shock equations with the addition of the $F/\rho u$ term to the energy equation. For combustion fronts (detonations and deflagrations) the corresponding term is Q, the specific heat of combustion. One

difference between the physics of heat fronts and that of combustion fronts is that for a heat front F is regarded as known *a priori* but the mass flux, ρu is not; for combustion Q is known. The equations are also similar to those describing astrophysical ionization fronts, but there the quantity usually regarded as known is the number flux of ionizing photons or equivalently the mass flux.

It is more convenient for many purposes (including comparison with results in books) to use the specific volume $V \equiv 1/\rho$ rather than the density in our discussion.

If we define the (constant) mass flux, $\rho u \equiv j$, then equations (1) and (2) can be combined to give the "Rayleigh line" of final states, so called because on a P vs V graph it is a straight line through (P_1, V_1) with slope $-j^2$. We have

$$\frac{P_2 - P_1}{V_2 - V_1} = -j^2 \tag{4}$$

We note that in the absence of the viscous dissipation of momentum, P_2 and V_2 can be replaced by P and V for all intermediate states inside the heat front as well. Equations (1), (2), and (3) may be combined to give the heat front Hugoniot:

$$F = \frac{1}{2}\sqrt{\frac{P_2-P_1}{V_1-V_2}}\left(\frac{\gamma_2+1}{\gamma_2-1}P_2V_2 - \frac{\gamma_1+1}{\gamma_1-1}P_1V_1 - P_2V_1 + P_1V_2\right) \tag{5}$$

where we have introduced an equation of state in the form $h = [\gamma/(\gamma - 1)]\, PV$. The schematic behavior of heat front Hugoniot curves is shown in Fig. 2 for two different values of F. The Hugoniot curve has two branches. The one extending toward high pressure has infinite slope at $P_1 = P_2$ and is asymptotic to $(\gamma_2 - 1)/(\gamma_2 + 1)$. The lower branch for $P_2 < P_1$ is asymptotic to $P_2/P_1 = 1$ and (unphysically) to $P_2/P_1 = (1 - \gamma_2)/(1 + \gamma_2)$. In the limit $F \rightarrow 0$ the two branches merge into the ordinary shock Hugoniot curve together with a horizontal line, $P_1 = P_2$. The curve then represents the three types of discontinuities allowed by the equations of motion: ordinary compressional shocks, unphysical (usually) rarefaction shocks, and so called "tangential" discontinuities ($P_1 = P_2$, $u_1 = u_2 = 0$, $\rho_1 \neq \rho_2$).

Equations (4) and (5) are essentially two equations in three unknowns; j, P_2, and V_2. (For the moment we regard F and the upstream quantities, P_1, and V_1., as known.) To make further

progress we must find an additional constraint from the physical conditions of the problem at hand.

Heat Fronts Driven by Soft, Thermal X-Rays in Particular: For the model problem considered the additional constraint is provided by the heat bath of Planckian radiation in which the gas finds itself as it exits the heat front:

$$T_2 = T_R \tag{6}$$

Our heat front would be constrained at this point if the radiative flux F_R arriving at the front were known. For the problem at hand, however, that is not precisely the case, even if we ignore any nonzero albedo as insignificant. The reason is that the hot gas is blowing off into a vacuum, and it is approximately isothermal. As we shall see in the next section this means that there will be, for times of interest, an isothermal similarity rarefaction (ISR) wave between the radiation source and the heat front. For an ideal gas, an ISR, in order to remain isothermal, requires a constant power input per unit cross sectional area of $P_2^{3/2}\ V_2^{1/2}$ where P_2 and V_2 are the values at the leading edge of the rarefaction wave. Again anticipating results of the next section, we have used the subscript 2 implying that conditions at the leading edge of the ISR are those at the exit side of the heat front. We therefore make the substitution $F_R = F_R^0 - P_2^{3/2}\ V_2^{1/2}$ in Eq. (5), yielding

$$F_R^0 = P_2^{3/2} V_2^{1/2} + \frac{1}{2}\sqrt{\frac{P_2-P_1}{V_1-V_2}}\left(\frac{\gamma_2+1}{\gamma_2-1}P_2V_2 - \frac{\gamma_1+1}{\gamma_1-1}P_1V_1 - P_2V_1 + P_1V_2 \right) \tag{7}$$

where $F_R^0 = \sigma T_R^4$ for now. The modified Hugoniot curve, Fig. 3, has similar behavior to the Hugoniot curve shown in Fig. 2 with two exceptions. First, the high pressure branch is asymptotic to $V_2/V_1 = 1/10$ (for $\gamma_2 = 5/3$); second, the upper part of the low pressure branch ends with zero slope at $V_2/V_1 = (F_R^0/P_1\sqrt{P_1V_1})^2$. The ideal-gas result for the ISR power consumption has been used because that is an excellent approximation for low-Z materials at soft X-ray temperatures with density less than a few g/cm^3. Hence we shall also rewrite Eq. (6) as

$$P_2 V_2 = \frac{R T_R}{\mu} \tag{8}$$

where R is the gas constant and μ is the fully ionized mean molecular weight, $\mu \equiv A/(Z+1)$.

We seek solutions then to Eqs. (7) and (8) for P_2 and V_2 given $F_R{}^0$, T_R, P_1, and V_1. Depending on the relative values of these last parameters there are (it can be shown) one, two, or four real, positive solutions to these equations, corresponding to the possible intersections of the appropriate isotherm with the appropriate modified Hugoniot curve (Eq.7).

Rather than proceed directly with an exhaustive discussion of the various solutions, we will use some physical arguments to determine the unique solutions physically possible in the context of our particular gas-dynamic problem. Because we shall be extensively concerned in what follows with the speeds at which various signals propagate, it is useful to define two more symbols: the adiabatic sound speed, $c \equiv \sqrt{(\partial P/\partial \rho)_s} \equiv V\sqrt{-(\partial P/\partial V)_s}$ and the isothermal sound speed, $a \equiv \sqrt{(\partial P/\partial \rho)_T} \equiv V\sqrt{-(\partial P/\partial V)_T}$.

Consider what we can infer from the constraint (8) that the final state (P_2, V_2) of the gas flowing through the heat front must lie on the T_R isotherm, c.f. Fig. 4. We note first that the part of the isotherm between points C and D is excluded since the mass flux, $j = [(P_2-P_1)/(V_1-V_2)]^{1/2}$, must be real, i.e. the slope of the Rayleigh line must be negative.

Next consider heat fronts resulting in a compression of the gas corresponding to points above C on the isotherm such as A, B, or O. For a given mass flux (a given Rayleigh line) there are in general two possible final states, points A and B for example. For final states above O, such as A, the exit speed of the gas from the heat front is less than the isothermal sound speed, $u_2 < a_2$. This follows immediately from the relative slopes of the Rayleigh line and the isotherm at point A:

$$u_2^2 = j^2 V_2^2 < \left|\frac{\partial P_2}{\partial V_2}\right|_{T_2} V_2^2 = a_2^2 \tag{9}$$

Conversely, for final states such as B between C and O, the exit speed is supersonic ($u_2 > a_2$); while for final state O it is sonic ($u_2 < a_2$). If the exit speed from our heat front were less than the isothermal sound speed, then the isothermal rarefaction downstream from the heat front would catch it and weaken the

compression until the exit speed was sonic ($u_2 \rightarrow a_2$). We conclude that the only compression heat fronts that can be physically realized in our situation have final states corresponding to points between O and C on the T_R isotherm. It can readily be shown that these correspond to compressions by a factor of 2 or less. Finally, all compression heat fronts for our problem propagate supersonically ($u_1 > c_1$) into the gas ahead of them. This follows from the fact that for our problem $T_2 >> T_1$ so that the possible Rayleigh lines are much steeper than the adiabat through (P_1, V_1). Therefore a compressional heat front cannot be preceded by a shock wave.

Finally consider expansion heat fronts corresponding to final states below D on the T_R isotherm. Using the same arguments as above we see that these fronts propagate subsonically into the gas ahead of them, ($u_1 < a_1$). And, following the above arguments, we see that final states such as E between D and O' have subsonic exit speeds ($u_2 < a_2$) while those below O' such as F have supersonic exit speeds ($u_2 > a_2$). Therefore final states between D and O' are impossible in our situation -- the isothermal rarefaction would catch them. But final states such as F below O' are also impossible! There are two reasons for this. First, the implied intermediate states of the gas are impossible for such a front. The thickness of a soft x-ray driven heat front must be of the order of a Planck mean free path for the photons providing the heat. It can readily be shown that molecular viscosity is a very small effect indeed in a front of that thickness, (photon mean free path >> electron or ion mfp), and that therefore all intermediate states of the gas within the heat front must lie on the Rayleigh line (no viscous term in the momentum equation). The state of the gas must vary continuously, and so in traversing the Rayleigh line to a state such as F must cross through a region between E and F in which $T > T_R$. This is impossible: there is no way to heat the gas to such temperatures.

The second reason that fronts having final states below O' are impossible is that they are absolutely unstable. Such a front is subject to (in one dimension) <u>five</u> independent perturbations: displacements of the front, entropy disturbances left behind in the gas behind the front, sound waves propagating ahead of the front, and, because $u_2 > a_2$, sound waves propagating both forward and backward in the gas behind the front. The front is absolutely unstable because its perturbations are subject to only <u>four</u> constraints; conservation of mass, momentum, and energy, and the imposed final temperature. We conclude that an expansion heat front must be "critical" in the sense that only final states O' at which the Rayleigh line is tangent to the T_R isotherm and for which the exit speed is exactly the isothermal sound speed, $u_2 = a_2$, are

possible. This condition is analogous to the Chapman-Jouget condition on a combustion front.

Now if F_R^0 is too small, and it falls like T_R^4, there may not be enough radiation flux to sustain the minimum mass flux through a compression heat front (c.f. Fig. 4); an expansion heat front may be the only course open. But we have concluded above that for a given P_1, V_1, and T_R that the final state is determined (point O in Fig. 4) -- the expansion heat front must be "critical." What if that final state (P_2, V_2) does not satisfy Eq. (7), i.e. does not lie on the appropriate Hugoniot? In general it will not; we need another free parameter, and it appears that we do not have any. The way out is to vary the initial state (P_1, V_1). We can show, in fact, that together the above constraints imply that the initial state (for a $\gamma = 5/3$ ideal gas) must lie on the curve shown in Fig. 5. Our expansion heat front is propagating subsonically into the gas ahead of it so it can be preceded by a shock or rarefaction. These are just the one parameter disturbances of the initial conditions that we need:

$$(P_0, V_0) \xrightarrow[\text{rarefaction}]{\text{shock or}} (P_1, V_1) \qquad (10)$$

From Fig. 5 note that for $T_R \gtrsim 100$ eV we have $P_1 \gtrsim 10$ Mbar. The solution with a rarefaction might be appropriate if a sufficiently strong shock had already compressed the material. Since our model problem involves previously undisturbed, ordinary terrestrial material, we shall be concerned with the solution in which a shock precedes an expansion heat front.

Table I summarizes the properties we have so far derived for the soft X-ray driven heat fronts appropriate to our model problem.

TABLE I

Compression heat fronts	Expansion heat fronts
$u_1 > c_1$ "supersonic"	$u_1 < a_1$ "subsonic"
$u_2 \geq a_2$	$u_2 = a_2$ "critical"
$0.5 \leq V_2/V_1 \leq 1$	$V_2/V_1 \geq 1$
$P_2/P_1 \geq 1$	$P_2/P_1 \leq 1$
Not preceded by anything	Preceded by shock or rarefaction

Complete Gas Flow Solutions: Up to this point in our development the only physical parameters we have been considering are P_0, ρ_0, F_R, and T_R. We make the usual dimensional-analysis argument that since these parameters cannot be combined to give length and time dimensions in any other combination than l/t, there are no effective length or time scales. This is, of course, not quite true. There are length and time scales associated with the opacity, and these do indeed introduce important effects (such as "transonic" heat fronts). However, we shall presently show that these scales are generally either much smaller or much larger than the length or time scales in which we are interested. For the moment, therefore, we shall look for similarity solutions such that all the gas dynamic flow variables are approximately functions of the single space-time variable x/t.

On an x-t diagram we expect the flow to look like that shown schematically in Fig. 6. Ignoring the pressure ahead of the heat front as negligible compared to that behind it, we combine Eq. (7) and (8) in the dimensionless form

$$\phi = p + \frac{p}{2\sqrt{p-1}}\left(\frac{\gamma_2+1}{\gamma_2-1} - p\right) \tag{11}$$

where $\phi \equiv F_R^0/[\rho_0(RT_R/\mu)^{3/2}]$ is a dimensionless flux and $p \equiv P_{max}/(\rho_0 RT_R/\mu)$ is a dimensionless pressure. P_{max} is the maximum pressure in the flow — in this case, the pressure between the heat front and the leading edge of the rarefaction (i.e. behind the heat front). The function $p(\phi)$, which Eq. (11) gives implicitly, is shown in Fig. 7.

It is a simple matter to use the equations of continuity and momentum conservation to derive some useful formulas for the velocities. The heat front propagates, relative to the material ahead of it, at a speed

$$\frac{v_c}{a} = \frac{p}{\sqrt{p-1}} \tag{12}$$

where $a = (RT_R/\mu)^{1/2}$. The heat front separates from the leading edge of the isothermal rarefaction wave at a speed

$$\frac{v_{sep}}{a} = \frac{1}{\sqrt{p-1}} - 1 \tag{13}$$

Equation (13) immediately implies that we should not consider solutions to Eq. (11) for $p > 2$, that is for $\phi < (\gamma_2 + 1)/(\gamma_2 - 1)$. Such solutions correspond to heat fronts which have exit speeds less than the isothermal sound speed and so cannot exist under the conditions of our problem. From its definition, p is also the factor by which matter is compressed in passing through a compression heat front. Hence follows our previous remark that such a heat front can give a compression no greater than a factor of two.

The flow previously described for an expansion (subsonic) heat front should look like that diagrammed in Fig. 8. We can assume that the pressure in the cold dense material ahead of the shock can be ignored, i.e. that the shock is very strong. However, we can in general make no such simplifying assumptions about flow variables on either side of the heat front. We have the additional constraint that the exit speed from the heat front must be equal to the isothermal sound speed, or equivalently that the Rayleigh line is tangent to the final isotherm. This constraint can be written

$$\frac{P_2 - P_1}{V_2 - V_1} = -\frac{P_2}{V_2} \tag{14}$$

Making the strong shock substitution, $V_1 = V_0(\gamma_1 - 1)/(\gamma_1 + 1)$ we combine Eqs. (7), (8) and (14) into the dimensionless form

$$\phi = p\left[\frac{\sqrt{R_1}}{\sqrt{R_1} + \sqrt{R_1 - p}}\left(\frac{R_2 - p}{2}\right) + 1\right] \tag{15}$$

where $Y_{1,2} \equiv (\gamma_{1,2} + 1)/(\gamma_{1,2} - 1)$ and again ϕ and p are the dimensionless flux and pressure as defined earlier. Here, the maximum pressure is achieved <u>ahead</u> of the heat front, between the heat front and the shock. The inversion of Eq. (15), $p(\phi)$, is shown in Fig. 7 for the case $\gamma_1 = \gamma_2 = 5/3$. A very good fit (to better than 3%) to the inversion of Eq. (15) for this case is

$$p \equiv \frac{9}{2}\left(1 - \sqrt{1 - \frac{2\phi}{9}}\right) \rightarrow \frac{\phi}{2} \text{ for small } \phi \tag{16}$$

Putting the dimensions back in the limiting form of Eq. (16) we have

$$P_{max} \rightarrow \frac{1}{2}\frac{\sigma T_R^4}{\sqrt{\frac{RT_R}{\mu}}} \tag{17}$$

demonstrating the $P \sim T_R^{3.5}$, P independent of ρ_0 , scaling expected from dimensional analysis, together with the correct numerical factors.

Again, it is straightforward to derive some useful velocity formulas. The shock propagates into the material ahead of it at a speed

$$\frac{v_s}{a} = \sqrt{\frac{pR_1}{R_1 - 1}} \tag{18}$$

The shock and heat front separate from each other at a relative speed

$$\frac{|v_s - v_e|}{a} = \sqrt{\frac{p}{R_1(R_1-1)}} + \sqrt{1-\frac{p}{R_1}} - 1 \qquad (19)$$

For small ϕ (small p), this speed is proportional to $p^{1/2}$. As T_R (and hence ϕ and p) increases, however, this separation speed reaches a maximum and then diminishes until for $p = 4(1 - 1/R_1)$ (corresponding to $\phi = R_2$) it vanishes, and the heat front keeps up with the shock.

As we have noted, $\phi = R_2$ is the critical value for compression heat fronts, and hence it is the critical value for the transition from the expansion-heat-front-plus-shock type of solution to the compression-heat-front-solution. For $\gamma_2 = 5/3$ this condition defines a critical radiation temperature for a particular material:

$$T_{R,\mathrm{crit}} = \left(\frac{4\rho_0}{\sigma}\right)^{2/5}\left(\frac{R}{\mu}\right)^{3/5} \qquad (20)$$

$$\left(\frac{T_{R,\mathrm{crit}}}{100\ \mathrm{eV}}\right) = 4.23\left(\frac{\rho}{1\ \mathrm{g/cm^3}}\right)^{2/5}\mu^{-3/5} \qquad (21)$$

There are limitations of the validity of self-similarity. In deriving a similarity solution we have been implicitly ignoring the fact that there are indeed length and time scale parameters associated with the opacity of the material being irradiated. For our problem it is often enough to consider the "Planck mean free path", l_P of the photons driving the heat front

$$l_P(\rho, T, T_R) \equiv \frac{\int \frac{B_\nu(T_R)}{\rho\kappa_\nu(\rho, T)}\, d\nu}{\int B_\nu(T_R)\, d\nu} \qquad (22)$$

as the scale parameter. Here $\kappa_\nu(\rho, T)$ is the opacity of matter at density ρ and temperature T to photons at frequency ν. The Planck mean free path is simply a useful estimate of how deep and over what depth range the incoming energy flux of radiation penetrates before being absorbed. Note that this is quite different from a

Rosseland mean free path which is only meaningful for $T = T_R$ and which uses a different weighting function, dB_ν/dT_R, which peaks at higher energy (about $4kT_R$) than $B_\nu(T_R)$.

As we have mentioned, we are able to ignore this length scale, l_P, because for times of interest (t from a few nanoseconds to a few tens of nanoseconds) it is either much smaller than or much greater than the other gas dynamic scale lengths of the problem. For illumination by soft X-rays, this property occurs only for low-Z materials. The opacity of these materials to soft X-rays is dominated in the fat part of the black body spectrum by photoionization from the K-shell of electrons, the energy threshold for K-shell photoionization being at ~ $13.6Z^2$ eV. In the matter just ahead of the heat fronts we have been considering, the temperature is low enough that the K-shell electrons are retained by the nuclei with $Z \geq 3$. This is true even though the matter may have been shock heated to tens of eV in the case of expansion heat fronts. However, the matter behind the heat front has been heated to ~ T_R, at which temperatures materials with $Z <\sim 6$ are fully stripped of electrons and the opacity drops by orders of magnitude. Now l_P for cold materials at their normal laboratory densities ranges from ~$9(T_R/100\text{ eV})^3$ μm for $^7Li^2H$ down to ~ $0.7(T_R/100\text{ eV})^3$ μm for C_XH_X. It is easy to calculate from the previous formulae in this section that after a few nanoseconds or even a few tenths of nanoseconds the relevant length scales of the problem, such as the distance by which the shock and an expansion heat front are separated, greatly exceed l_P in the shocked matter. (This is not true if T_R is near T_{crit} as we discuss in the next section.) It is likewise straightforward to use the formulas together with the Saha equation to estimate the Planck mean optical depth of the matter at ~ T_R behind the heat front and find that it is small for times ranging from several tens of nanoseconds for LiH to several nanoseconds for C_XH_X.

The dramatic change in opacity to soft X-rays at the heat front is what limits this whole analysis to low-Z materials. Retaining (at least) their K-shell electrons at soft X-ray temperature, high-Z materials retain their opacity and there is no significant time other than the initial penetration when radiation is not diffusing into these materials. The assumption of a steady heat front with a steady flux of radiation incident on it then breaks down.

III. SOME TIME-DEPENDENT HEAT FRONT EFFECTS

"Transonic" Heat Fronts: When the X-rays are first incident on cold, dense matter they propagate forward at the speed of light until they are stopped in a region about one Planck mean free path

thick. This region heats to a matter temperature T with a characteristic heating time

$$t_h = \frac{\frac{3}{2}\left(\frac{\rho_0 RT}{\mu}\right) l_P}{\sigma T_R^4} \tag{23}$$

and expands with a characteristic time (sound crossing time)

$$t_{ex} = \frac{l_P}{\sqrt{\frac{RT}{\mu}}} \tag{24}$$

The ratio of these times

$$\frac{t_{ex}}{t_h} = \frac{2}{3}\left(\frac{T_R}{T}\right)^{3/2}\phi \tag{25}$$

roughly indicates which process is most rapid. For the temperatures and materials we are concerned with here, we have $\phi >\sim 0.3$, and we see that the matter heats up to a substantial fraction of T_R before expansion and adiabatic cooling can slow up the heating rate. (It is interesting to note that the heating time to T_R is approximately independent of T_R since $l_P \propto T_R^3$.

At these very early times our unsteady heat front is propagating supersonically. The question is whether the pressures being generated in it will form a shock wave that can propagate through it and get ahead of it. The answer is presumably no for $\phi > 4$. For $\phi < 4$ we expect that eventually a distinct shock wave will break out ahead of the heat front. This can take a while, however, because Eq. (19) shows that an expansion heat front and the shock it spawns ahead of it have a maximum separation speed at $p \approx 2$ ($\phi \approx 3$). As ϕ (which is proportional to $T_R^{5/2}$) increases further toward the limiting value of 4 the separation speed declines to zero. Unless the shock and heat front are separated by at least a Planck mean free path they cannot really be said to have a separate existence. Therefore a reasonable lower limit to the time required for the gas dynamic flow to "relax" to the similarity solution of shock plus expansion heat front, described previously, is

$$t_{trans} = \frac{l_P\ (\rho=\rho_0, T=0)}{|v_s - v_e|} \qquad (26)$$

(which formally diverges as $\phi \rightarrow 4$ from below). In this "transonic" heat front situation the front can take a very long time to relax from its initially supersonic propagation toward a steady state. (So long, in fact, that albedo effects become important and the front is never steady.)

"Reflected" Flux Effects: Finally we shall stop sweeping under the rug the fact that the hot ($\sim T_R$) blowoff material in the flow can lose energy by radiation that escapes to $x = +\infty$. This effect is cumulative with time as the optical depth of the blowoff increases. It causes a lowering of the flux actually reaching the heat front and, therefore, in the pressure the flux generates. We describe below a reasonable way to estimate this effect for the expansion heat front case. The other case can be analyzed similarly.

First, no matter how optically thick it is, a region cannot emit a thermal radiation flux greater than σT_R^4; and unless the flux emitted is comparable to σT_R^4 it has little effect on the heat front. Hence we ignore regions with $T < T_R$ (e.g. the heat front itself and shocked material).

Within the framework of our theory the outgoing (to + ∞, cf. Fig. 1) flux, F_{refl}, can be estimated by integrating the equation of radiative transfer through the ISR. This can be done because $\rho(x,t)$ is known in terms of the exit density from the heat front, and the temperature is $\sim T_R$. Hence one can use hydrogenic bound-free and free-free opacities together with the Saha equation (the low-Z matter is very nearly fully ionized) to estimate the optical depth of the ISR. The standard formula below gives the emergent flux:

$$F_{refl} = \pi \int_0^\infty B_\nu(T_R)\ [1-2E_3(\tau_\nu)]\ d\nu \qquad (27)$$

Where τ_ν is the optical depth of the ISR at frequency ν and E_3 is an exponential integral,

$$E_3(x) \equiv \int_1^\infty \frac{e^{-xt}}{t^3} dt \qquad (28)$$

One then can use $F_R^0 = \sigma T_R^4 - F_{refl}$ to make a first-order estimate of how the ablation pressure diminishes with time.

Acknowledgments

This work was performed under the auspices of the U.S. Department of Energy by Lawrence Livermore National Laboratory under contract No. W-7405-Eng-48.

Figure Captions

1. The model problem is a slab of cold, dense, low-Z matter suddenly illuminated on one side by thermal X-radiation at time $t = 0$.

2. Heat front Hugoniot curves for two different values of the driving flux, assuming $\gamma_1 = \gamma_2 = 5/3$.

3. Heat front Hugoniot curves, modified to account for flux loss in an isothermal similarity rarefaction wave, for two different driving flux values, assuming $\gamma_1 = \gamma_2 = 5/3$.

4. P, V diagram showing various possible transitions from an initial (P_1, V_1) state to states on a higher temperature isotherm ($T_2 = T_R$).

5. Required upstream (P_1, V_1) conditions for "critical" expansion heat front. (The dashed portion of the curve corresponds to $T_R > T_{crit}$, and is not physically possible for the model problem considered).

6. Space time diagram for a compression (supersonic) heat front.

7. Maximum pressure achieved for both expansion and compression heat fronts as a function of the driving flux.

8. Space time diagram for an expansion (subsonic) heat front.

References

1. R. E. Marshak, *Phys. Fluids* **1**, 24 (1958)

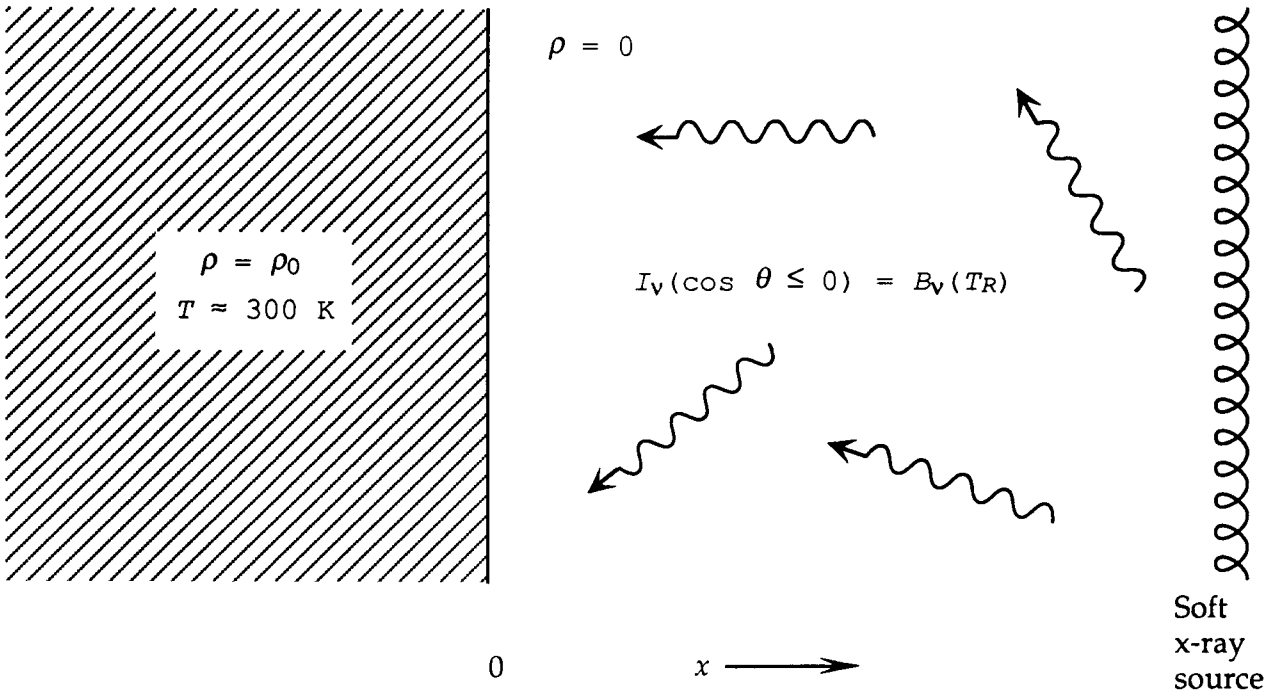

Fig. 1 The model problem is a slab of cold, dense, low-Z matter suddenly illuminated on one side by thermal X-radiation at time t=0.

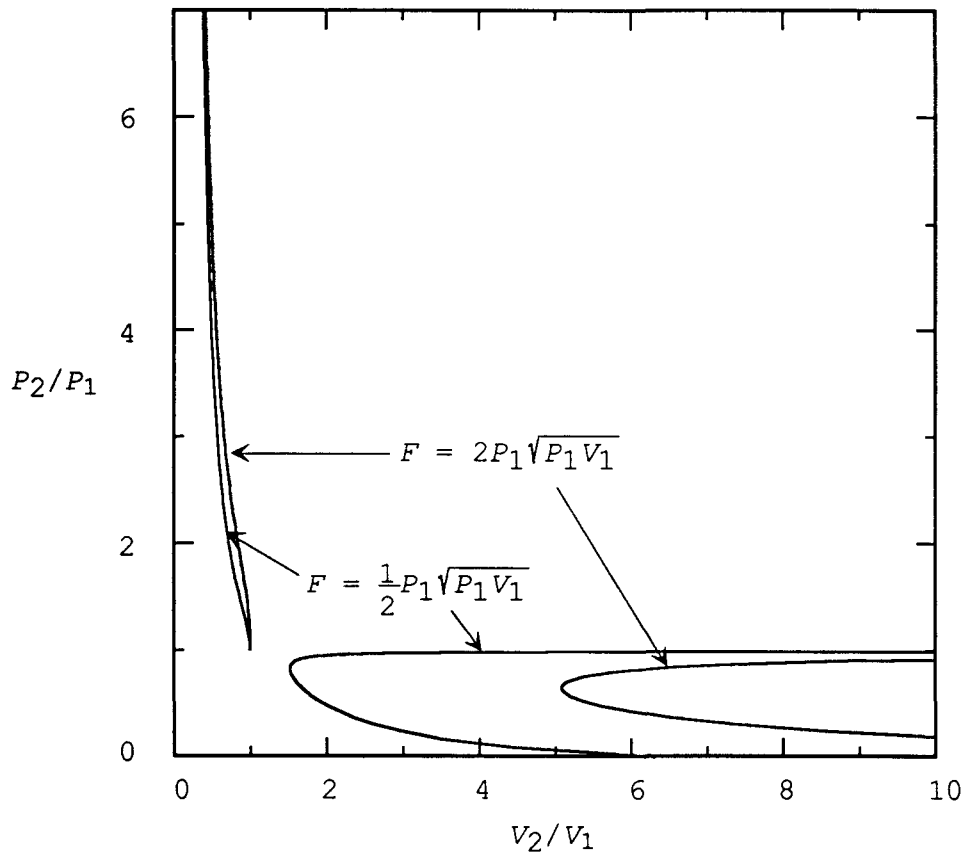

Fig. 2 Heat front Hugoniot curves for two different values of the driving flux, assuming $\gamma_1 = \gamma_2 = 5/3$.

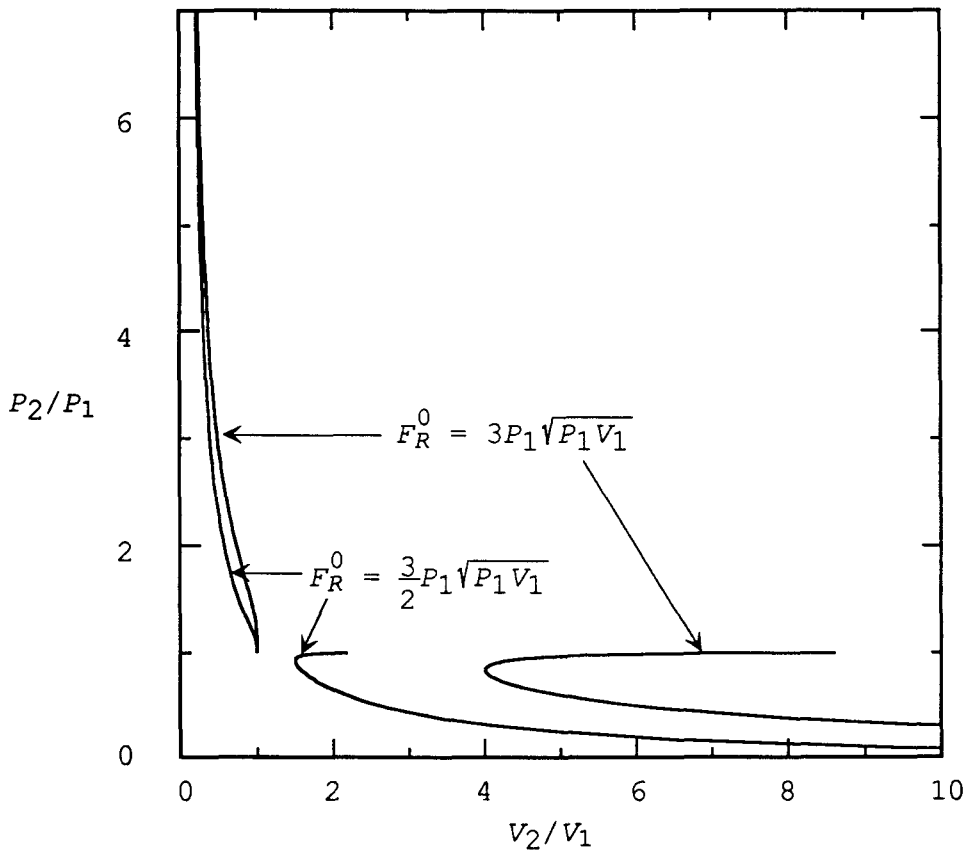

Fig. 3 Heat front Hugoniot curves, modified to account for flux loss in an isothermal similarity rarefaction wave, for two different driving flux values, assuming $\gamma_1 = \gamma_2 = 5/3$.

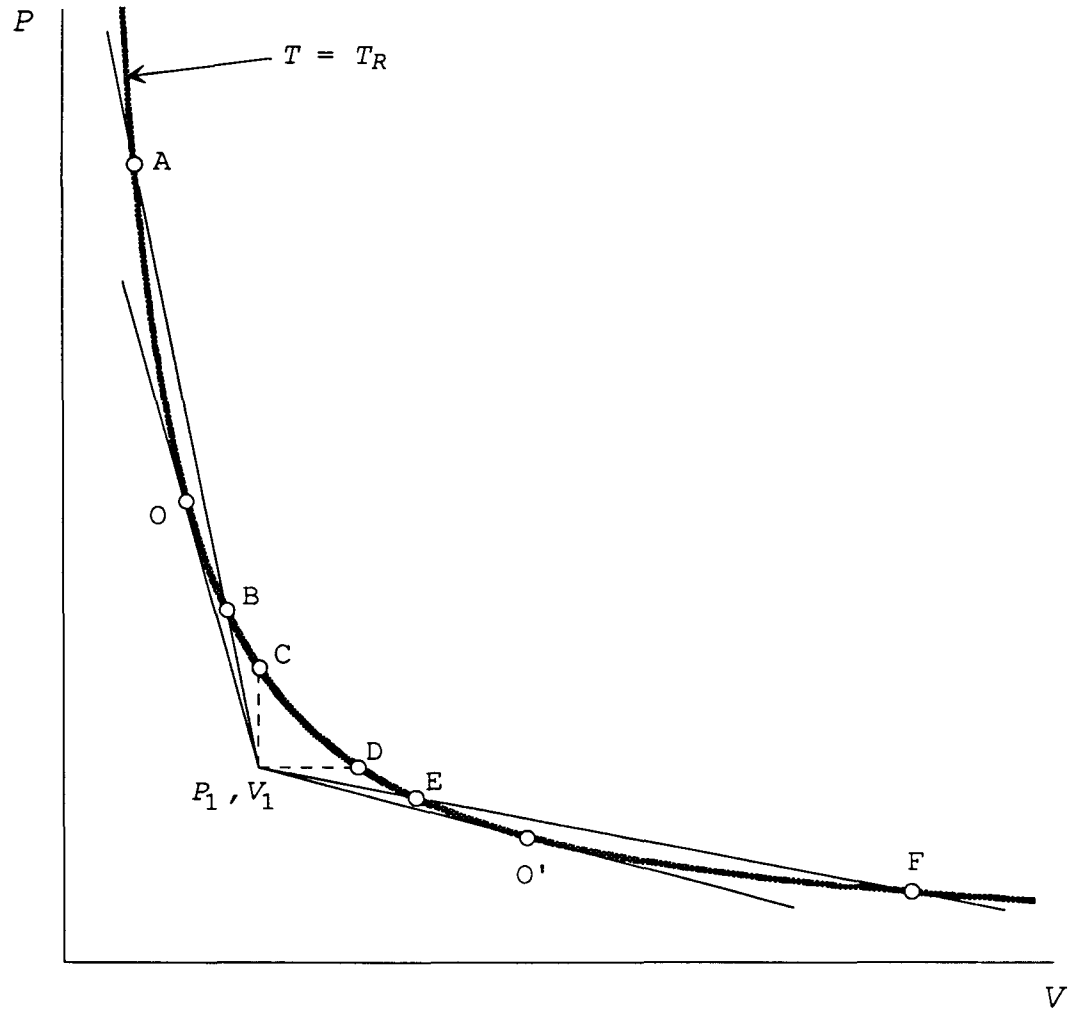

Fig. 4 *P*, *V* diagram showing various possible transitions from an initial (P_1, V_1) state to states on a higher temperature isotherm ($T_2 = T_R$).

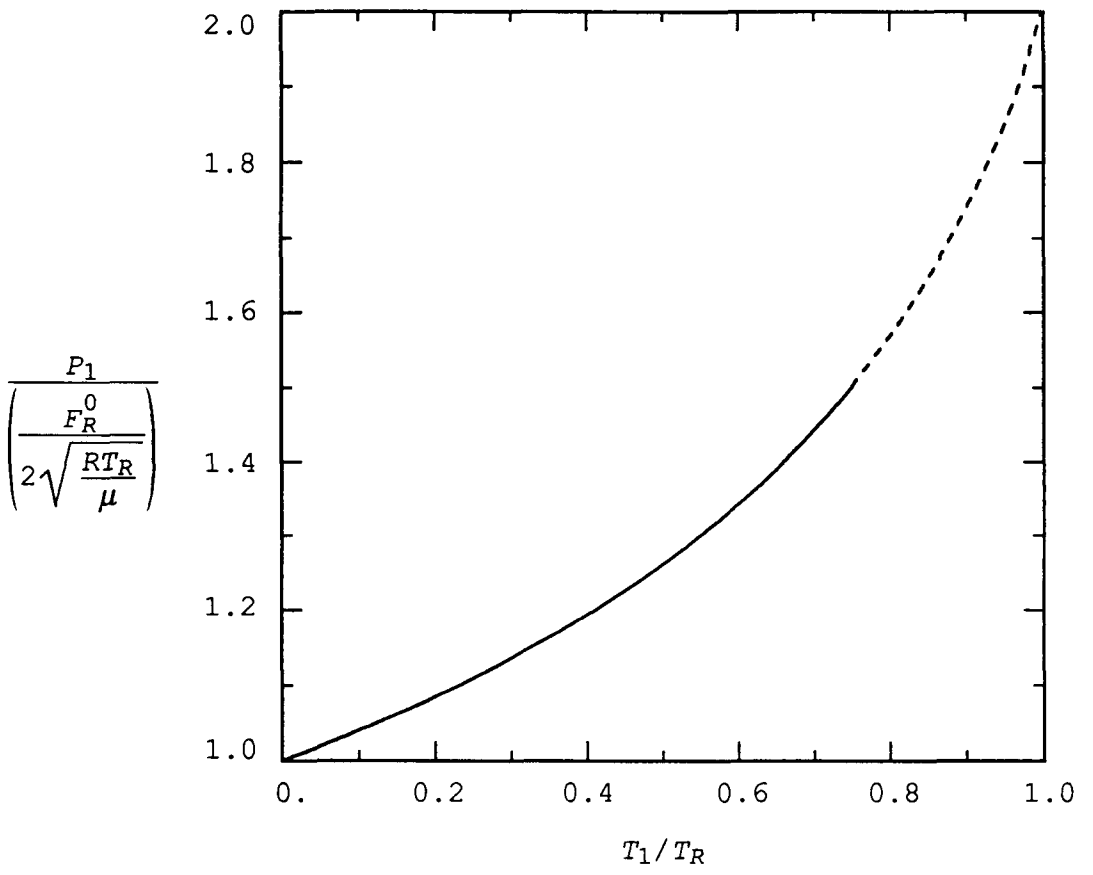

Fig. 5 Required upstream (P_1, V_1) conditions for a "critical" expansion heat front. (The dashed portion of the curve corresponds to $T_R > T_{crit}$, and is not physically possible for the model problem considered.)

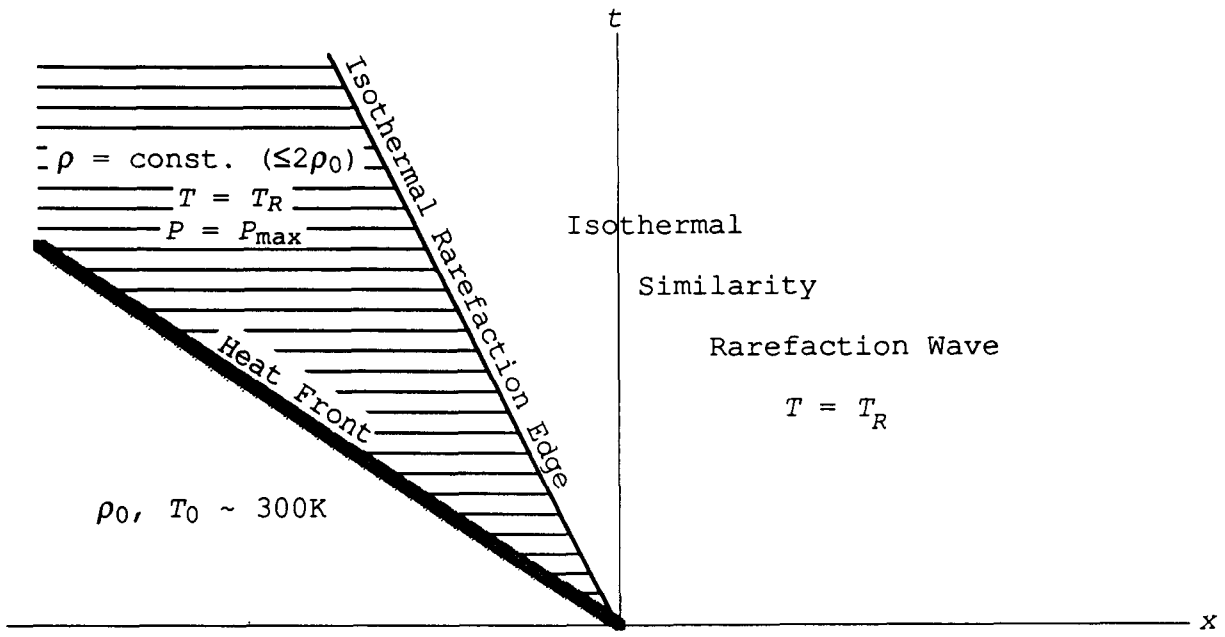

Fig. 6 Space time diagram for a compression (supersonic) heat front.

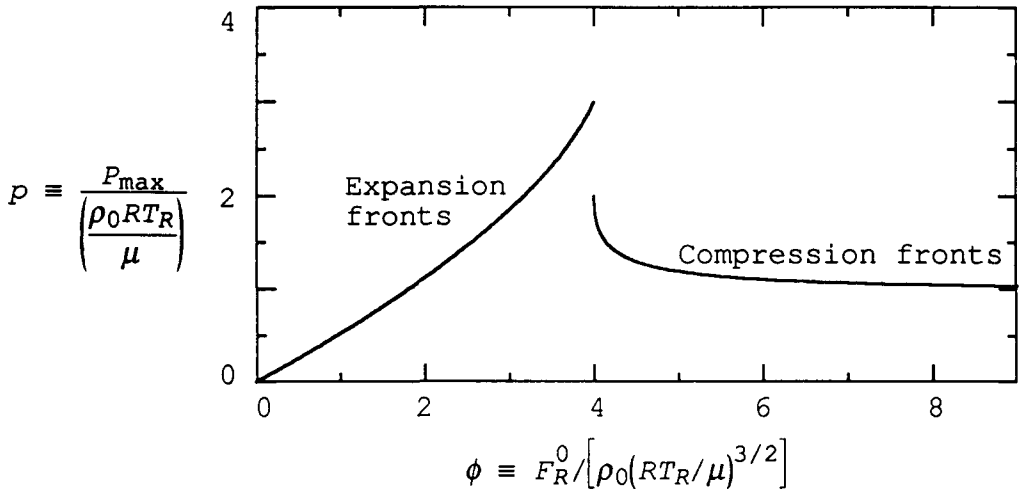

Fig. 7 Maximum pressure achieved for both expansion and compression heat fronts as a function of the driving flux.

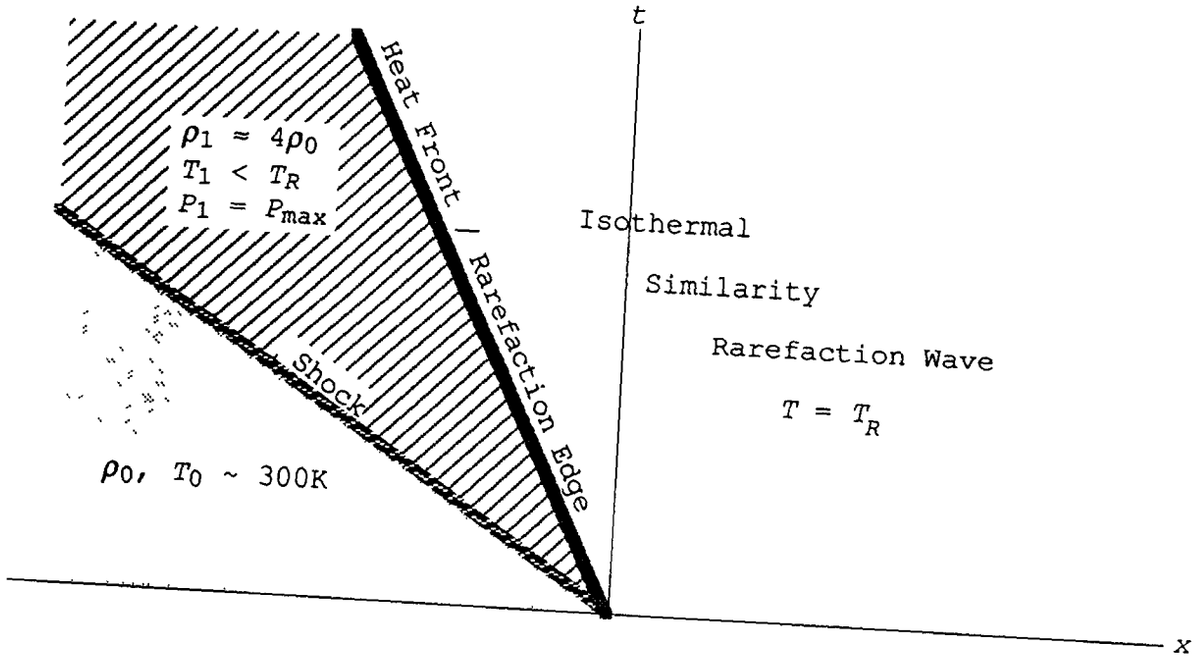

Fig. 8 Space time diagram for an expansion (subsonic) heat front.